Proceedings of the ASME 2018 37th International Conference on Ocean, Offshore and Arctic Engineering
OMAE 2018
June 17 –22, 2018, Madrid, Spain

OMAE2018-77589

VERIFICATION OF A NUMERICAL MODEL OF THE OFFSHORE WIND TURBINE FROM THE ALPHA VENTUS WIND FARM WITHIN OC5 PHASE III

Wojciech Popko,[1] **Matthias L. Huhn**,[1] **Amy Robertson**,[2] **Jason Jonkman**,[2] **Fabian Wendt**,[2] **Kolja Müller**,[3] **Matthias Kretschmer**,[3] **Fabian Vorpahl**,[4] **Torbjørn Ruud Hagen**,[5] **Christos Galinos**,[6] **Jean-Baptiste Le Dreff**,[7] **Philippe Gilbert**,[8] **Bertrand Auriac**,[9] **Francisco Navarro Víllora**,[10] **Paul Schünemann**,[11] **Ilmas Bayati**,[12] **Marco Belloli**,[12] **Sho Oh**,[13] **Yoshitaka Totsuka**,[14] **Jacob Qvist**,[15] **Erin Bachynski**,[16] **Stian Høegh Sørum**,[16] **Paul E. Thomassen**,[17] **Hyunkyoung Shin**,[18] **Felipe Vittori**,[19] **Josean Galván**,[20] **Climent Molins**,[21] **Paul Bonnet**,[22] **Tjeerd van der Zee**,[23] **Roger Bergua**,[24] **Kai Wang**,[24] **Pengcheng Fu**,[25] **Jifeng Cai** [25]

[1]Fraunhofer Institute for Wind Energy Systems IWES, Division Wind Turbine and System Technology, 27572 Bremerhaven, Germany
wojciech.popko@iwes.fraunhofer.de

[2]National Renewable Energy Laboratory, Golden, CO, USA, [3]University of Stuttgart, Stuttgart Wind Energy, Stuttgart, Germany, [4]Senvion, Osnabrück, Germany, [5]OWEC Tower AS, Oslo, Norway, [6]Technical University of Denmark, Department of Wind Energy, Roskilde, Denmark [7]Electricité de France, Recherche et Développement, Palaiseau, France, [8]IFP Energies Nouvelles, Solaize, France, [9]Principia, La Ciotat, France, [10]Siemens Gamesa Renewable Energy, Hamburg, Germany, [11]University of Rostock, Endowed Chair of Wind Energy Technology, Rostock, Germany, [12]Politecnico di Milano, Department of Mechanical Engineering, Milano, Italy, [13]Nippon Kaiji Kyokai, Tokyo, Japan, [14]Wind Energy Institute of Tokyo Inc., Tokyo, Japan, [15]4Subsea, Hvalstad, Norway, [16]Norwegian University of Science and Technology, Department of Marine Technology, Trondheim, Norway, [17]Simis AS, Trondheim, Norway, [18]University of Ulsan, School of Naval Architecture and Ocean Engineering, Ulsan, The Republic of Korea, [19]National Renewable Energy Centre, Sarriguren, Spain, [20]TECNALIA, Derio, Spain, [21]Polytechnic University of Catalonia, Barcelona, Spain, [22]Siemens Industry Software, Cornellà de Llobregat, Spain, [23]Knowledge Centre WMC, Wieringerwerf, The Netherlands, [24]Envision Energy Limited, Shanghai, China, [25]China General Certification Center, Beijing, China

ABSTRACT

The main objective of the Offshore Code Comparison Collaboration Continuation, with Correlation (OC5) project, is validation of aero-hydro-servo-elastic simulation tools for offshore wind turbines (OWTs) through comparison of simulated results to the response data of physical systems. Phase III of the OC5 project analyzes the Senvion 5M wind turbine supported by the OWEC Quattropod from the alpha ventus offshore wind farm. This paper shows results of the verification of the OWT models (code-to-code comparison). A subsequent publication will focus on their validation (comparison of simulated results to measured physical system response data). Based on the available data, the participants of Phase III set up numerical models of the OWT in their simulation tools. It was necessary to verify and to tune these models. The verification and tuning were performed against an OWT model available at the University of Stuttgart – Stuttgart Wind Energy (SWE) and documentation provided by Senvion and OWEC Tower. A very good match was achieved between the results from the reference SWE model and models set up by OC5 Phase III participants.

INTRODUCTION

The Offshore Code Comparison Collaboration Continuation, with Correlation (OC5) project [1], which operates under the International Energy Agency (IEA) Wind Task 30 is the follow-up project of OC3 and OC4, which ran from 2005 to 2009

and from 2010 to 2014, respectively. The focus of OC3 and OC4 was to verify and benchmark simulation tools for offshore wind turbines (OWTs) with an emphasis on support structures through code-to-code comparison. This verification work led to dramatic improvements in model accuracy, which is a crucial achievement as the advancement of the offshore wind industry is closely tied to the development and accuracy of aero-servo-hydro-elastic OWT models [2, 3]. Participants of OC3 and OC4 expressed great interest in creating an extension to IEA Task 30 to focus on validating offshore wind modeling tools against experimental and/or in-situ data.

The OC5 project is focused on validation of aero-hydro-servo-elastic simulation tools for OWTs through comparison of simulated results to the response data of physical systems. OC5 is organized in three phases jointly coordinated by the National Renewable Energy Laboratory (NREL) from the USA and the Fraunhofer Institute for Wind Energy Systems IWES (IWES) from Germany. While the first two phases dealt with physical response data from tank tests [4, 5], Phase III aims to use open-ocean data for the validation work. Such data are obtained from alpha ventus—the first German offshore wind farm. Alpha ventus is located in the North Sea at the site of the average water depth of 28 m, around 45 km north of the Borkum island, as shown in Fig. 1.

FIGURE 1: LOCATION OF THE OWT WITHIN THE ALPHA VENTUS WIND FARM—MODIFIED SKETCH FROM [6]

Senvion[1] from Germany supported Phase III with data necessary to set up the turbine and the tower models, and with all necessary control settings that would allow running benchmark exercises on validation of simulation tools. OWEC Tower[2] from Norway provided the jacket support structure design data, including the transition piece (TP), foundation, and soil properties. The OWT schematic is shown in Fig. 2.

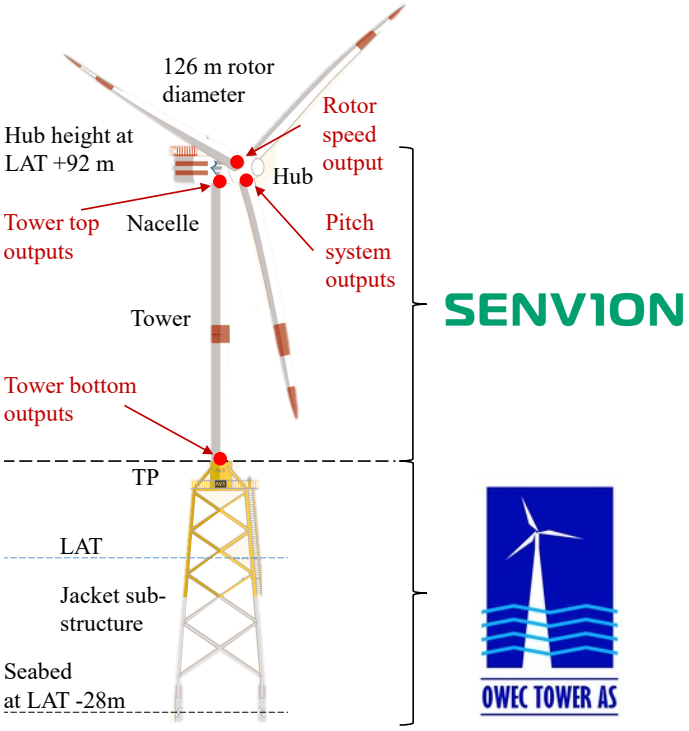

FIGURE 2: THE SENVION 5M TURBINE WITH THE JACKET SUPPORT STRUCTURE FROM OWEC TOWER—MODIFIED SKETCH FROM [7]

This paper shows results of the verification of the OWT models (code-to-code comparison) prior to their validation (comparison of simulated results to measured physical system response data). Based on the available data, the OC5 Phase III participants set up numerical models of the Senvion 5M turbine with the jacket support structure in their simulation tools. It should be noted that the OC5 Phase III participants have access to limited data of the OWT due to intellectual property (IP) reasons—the full definition of the controller, and detailed structural and aerodynamic properties of the blades could not be disclosed. Therefore, it was necessary to:

- Adapt controller and blades from a generic turbine model of the same power class that is available in the public domain,
- Build OWT models consisting of the OWEC Tower support structure, Senvion 5M turbine, and adapted generic controller and generic blades,

[1] https://www.senvion.com/global/en/

[2] https://www.owectower.no

- Verify and tune these OWT models prior to their validation,
- Answer the question whether those simplified OWT models—with adapted controller and blades—are sufficient for validation of a complex offshore system.

The verification and tuning was performed against an OWT model implemented in Flex5-Poseidon by the University of Stuttgart—Stuttgart Wind Energy (SWE), and documentation provided by Senvion and OWEC Tower. The OWT model from SWE contains structural and aerodynamic properties of the real blades, and the fully functional controller that could not be disclosed to the OC5 Phase III participants. The SWE model was extensively validated by Kaufer [8] and Müller [9] within the Research at alpha ventus (RAVE) projects—Offshore-Windenergieanlagen (OWEA), and OWEA Loads [10], respectively. Therefore, it can be considered as a reference model for the verification of other numerical models prior to their validation in Phase III.

A number of academic and industrial project partners from 11 countries participate in the task. Those actively involved in Phase III are listed in Tab. 1.

A set of state-of-the-art simulation tools for OWT modeling is represented in Phase III of the OC5 project. Table 2 summarizes some of their simulation capabilities that are important for verification of OWT models in Phase III. It should be noted that hydrodynamic capabilities are not listed herein, as the verification procedure was focused on the structural dynamics, aerodynamics, and the turbine controller.

TABLE 1: PARTICIPANTS OF OC5 PHASE III AND THEIR TOOLS

Organization full name	Abbreviation	Country	Tool
4Subsea	4S	Norway	ASHES
National Renewable Energy Centre	CENER	Spain	FAST V8
China General Certification Center	CGC	China	Bladed V4.8
Nippon Kaiji Kyokai	ClassNK	Japan	NK-UTWind
Technical University of Denmark – Department of Wind Energy	DTU	Denmark	HAWC2
Electricité de France – Recherche et Développement	EDF R&D	France	FAST V8
Envision Energy Limited	ENVISION	China	SAMCEF Wind Turbines 17.1 (SWT)
IFP Energies Nouvelles	IFPN	France	DeepLinesWind - V5R2
Fraunhofer Institute for Wind Energy Systems IWES – Division Wind Turbine and System Technology	IWES	Germany	MoWiT
National Renewable Energy Laboratory	NREL	USA	FAST V8
Norwegian University of Science and Technology – Department of Marine Technology	NTNU-M	Norway	SIMA
OWEC Tower	OWEC	Norway	–
Politecnico di Milano – Department of Mechanical Engineering	POLIMI	Italy	FAST V8
Principia	PR	France	DeepLinesWind - V5R2
Senvion	Senvion	Germany	–
Siemens Gamesa Renewable Energy	SGRE	Germany	SAMCEF Wind Turbines 17.1 (SWT)
Simis AS	SIMIS	Norway	ASHES
Siemens Industry Software	SISW	Spain	SAMCEF Wind Turbines 17.1 (SWT)
University of Stuttgart – Stuttgart Wind Energy	SWE	Germany	Flex5-Poseidon, Simpack
TECNALIA	TECNALIA	Spain	FAST V8
University of Ulsan – School of Naval Architecture and Ocean Engineering	UOU	The Republic of Korea	FAST V8
Polytechnic University of Catalonia	UPC	Spain	FloaWDyn
University of Rostock – Endowed Chair of Wind Energy Technology	URO	Germany	SiWEC
Wind Energy Institute of Tokyo Inc.	WEIT	Japan	FAST V8
Windrad Engineering GmbH	Windrad	Germany	SiWEC
Knowledge Centre WMC	WMC	The Netherlands	FOCUS6 Offshore

DEFINITION OF OFFSHORE WIND TURBINE

A description of the numerical model of the OWT consisting of the rotor-nacelle assembly (RNA), the tower, the TP, the jacket substructure, its foundation piles, and soil properties was set up at Fraunhofer IWES by Popko [11] based on the data provided by Senvion and OWEC Tower. The document does not suggest one modeling approach, as different simulation tools have different levels of complexity and features. Phase III participants chose how to interpret these data to best suit their simulation tools. The OWT and its basic dimensions are shown in Fig. 2. Note that the jacket piles are not visualized in this figure.

The complexity of the OWT model should be adequate for the foreseen validation task. On the other hand, it should be relatively simple to minimize the implementation effort and modeling errors in various simulation tools. Furthermore, not all design data could be released to the project participants due to the IP issues.

Controller

The full definition of the Senvion 5M turbine controller including the controller dynamic-link library (DLL), which is a standard input parameter to simulation tools, could not be disclosed to the OC5 Phase III participants due to IP issues. Therefore, Fraunhofer IWES decided to adapt the baseline NREL 5-MW turbine controller for Phase III needs. Basic control parameters were tuned to match dynamic behavior of the reference OWT model with the full Senvion 5M controller, which was available for comparison at SWE. The tuning was focused on two operating regions: (1) the variable speed region for optimal power tracking below the rated wind speed, and (2) the constant power region above the rated wind speed. All parameters that were tuned are listed in [11]. Alternatively, participants of Phase III could utilize control strategies suggested in [11] to implement their own controller.

Blades

Detailed structural and aerodynamic properties of the blades (mass, stiffness, chord, thickness, twist distribution, airfoil polars, etc.) could not be disclosed to the participants of Phase III. Therefore, it was required to tune the existing blades of the

TABLE 2: OVERVIEW OF SIMULATION CAPABILITIES OF TOOLS USED WITHIN PHASE III

Tool	Structural (elastic)	Aerodynamics (aero)	Control (servo)
ASHES	FEM, Euler-Bernoulli	BEM + Glauert correction + Prandtl tip and hub loss, DS	DLL, UD
Bladed V4.8	MBS + flexible modally reduced bodies, Timoshenko	BEM + Glauert correction + Prandtl tip and hub loss + skew inflow correction	DLL, UD
DeepLinesWind - V5R2	FEM, Mindlin	BEM + Glauert correction + Prandtl tip and hub loss + skew inflow correction, relaxation of induction factors	DLL
FAST V8	Substructure: FEM + Craig-Bampton, Timoshenko, Turbine: FEM preprocessor + Modal/MBS, Euler-Bernoulli, Blades: FEM, Timoshenko	BEM + Glauert correction + Prandtl tip and root losses + Pitt and Peters skewed wake	DLL, UD
Flex5-Poseidon	FEM + Modal	BEM or GDW + DS	DLL, UD
FloaWDyn	MBS/FEM, Euler-Bernoulli	(Aerodyn module) BEM + Glauert correction + Prandtl tip and root losses	DLL, UD
FOCUS6 Offshore	FEM, Timoshenko	BEM + Wilson and Lissaman correction + Prandtl tip and root losses	DLL, UD
HAWC2	MBS/FEM/stiffness-proportional Rayleigh damping, Timoshenko	BEM with 'Madsen and Larsen' correction for shear and dynamic inflow, Glauert and Coleman modification for skewed inflow and dynamic stall	DLL
NK-UTWind	FEM, Euler-Bernoulli	BEM (AeroDyn14)	DLL
MoWiT	MBS/FEM/modal reduced bodies, Euler-Bernoulli	BEM + Glauert correction + Prandtl tip and hub loss + skew inflow correction, relaxation of induction factors	DLL
SAMCEF Wind Turbines 17.1 (SWT)	FEM/MBS, Timoshenko	BEM + DS + Glauert correction + Prandtl tip and hub loss + dynamic wake + skew inflow + relaxation of induction factors	DLL, UD
SIMA	FEM, Euler-Bernoulli with shear correction	BEM + Glauert correction + Prandtl tip loss + skew inflow correction + Øye correction for dynamic stall and inflow	DLL, UD
Simpack	MBS, modal reduced FEM, Timoshenko	BEM + Glauert correction + Prandtl tip and root losses + Pitt and Peters skewed wake	DLL
SiWEC	MBS/FEM, modal reduced, Euler-Bernoulli	BEM + Glauert correction + Prandtl tip loss + skew inflow correction + Øye correction for dynamic stall	DLL, UD

BEM – blade element momentum
DLL – dynamic-link library
DS – dynamic stall implementation
FEM – finite element method
GDW – generalized dynamic wake
MBS – multibody-dynamics formulation
Modal – modal reduced system
UD – user-defined subroutine

NREL 5-MW offshore baseline turbine [12] to obtain a comparable structural response to the real blades that are used for the Senvion 5M turbine. Blade mass and stiffness distributions were tuned to achieve the first two flap- and edgewise eigenfrequencies of the real blade that were provided to the OC5 Phase III participants by Senvion. The remaining structural and aerodynamic properties were taken from the NREL 5-MW turbine definition [12]. Such an approach can be justified because: (1) the gross properties of the NREL 5-MW model were established based on the Senvion 5M turbine, and (2) the Senvion 5M turbine utilizes blades that were manufactured by LM Wind Power—the company that helped to establish the structural properties of the blades used in the Dutch Offshore Wind Energy Converter Project [13], which later on were adapted for the NREL 5-MW turbine. Therefore, the basic properties such as the length, mass, center of gravity, and damping ratio of the NREL 5-MW turbine blades and the blades from LM Wind Power used for the Senvion 5M turbine, are similar.

It must be emphasized that due to the differences in blade aerodynamics between the tuned NREL 5-MW blades (utilized in OC5 Phase III) and Senvion 5M reference turbine model (available for comparison at SWE), it was not possible to obtain a comparable system response at all operating regions of the turbine. Therefore, verification and validation could only be performed at certain ranges of operating wind speeds, as further described in the results section of this paper. It should be noted that tuning of the NREL blade aerodynamic properties in order to achieve a similar response to the real blade in all operating conditions would be very time consuming, and therefore not doable within the time frame of Phase III.

Jacket substructure

The following assumptions were made in modeling the jacket substructure:

- At joints, the connecting nodes of elements were defined at the intersection points of the members centerlines. This leads to overlap of elements in the analyzed jacket substructure.
- The local joint flexibility (LJF) was not modeled in the jacket substructure. Beam elements were simply clamped at the intersection of the centerlines of a joint's tubular members. Different tools have different modeling capabilities for the LJF, which would lead to additional uncertainties in the results interpretation. More detailed description on the current state of practice for modeling joints in space frame support structures can be found in [14].
- The TP was modeled with massless beam elements. Its mass was accounted for by three point masses. Note that the real TP is a complex structure that consists of many non-cylindrical elements. Therefore, modeling of its exact geometry would not even be possible in many of the simulation tools.
- The secondary steel masses of the jacket substructure, such as pile stoppers, cathodic protection, J-tubes, cables, crane, and boat landing platform were modeled as point masses applied at certain structural nodes and as redistributed masses by increasing the material density of certain jacket members.
- Impact of corrosion in terms of the reduced material stiffness or material thickness is not accounted for. The model will subsequently be validated against the measurements that were recorded around 1 year after deployment of the structure. During that time period, there was no significant development of corrosion.

DEFINITION OF LOAD CASES

Four groups of load cases (LCs) of increasing complexity were defined for stepwise comparison of results and tracing back potential errors from the implementation of OWT models in different simulation tools. Table 3 lists all verification LCs that were simulated in Phase III. A detailed description of these LCs can be

found in [15]. A similar stepwise approach for model verification was already adapted in the OC3 and OC4 projects [16, 17].

TABLE 3: OVERVIEW OF VERIFICATION LOAD CASES

Load Case	Enabled DOFs	Wind Conditions	Simulation Conditions
1a	Flexible RNA and tower, locked rotor, 6 DOFs constrained at tower bottom	No air	$\theta = 0$ deg, $\phi = 0$ deg – first blade points upwards
1b	Flexible RNA, tower, TP and jacket substructure, locked rotor, 6 DOFs constrained at LAT -29.5 m at 4 jacket legs	No air	as in LC 1a
1c	Flexible RNA, tower, TP, jacket substructure and foundation piles, locked rotor, elastic foundation model, 6 DOFs constrained at the bottom of 4 foundation piles	No air	as in LC 1a
2a	Flexible RNA and tower, 6 DOFs constrained at tower bottom	No air	Eigenanalysis, $\theta = 0$ deg, $\phi = 0$ deg – first blade points upwards
2b	Flexible RNA, tower, TP and jacket substructure, 6 DOFs constrained at LAT -29.5 m at 4 jacket legs	No air	as in LC 2a
2c	Flexible RNA, tower, TP, jacket substructure and foundation piles, elastic foundation model	No air	as in LC 2a
2d	Flexible jacket substructure and TP, rigid tower and RNA, 6 DOFs constrained at LAT -29.5 m at 4 jacket legs	No air	as in LC 2a
3.1	Rigid RNA and tower, 6 DOFs constrained at tower bottom, 1 rotational DOF for rotor, 1 rotational DOF for pitch mechanism	Steady, deterministic wind, changing from $V_{\text{cut-in}} = 3$ m/s to $V_{\text{cut-out}} = 30$ m/s with step of 1 m/s lasting for 50 s, no wind shear	Power production, periodic time series solution, $T = 1400$ s
3.2a seed 1–6	as in LC 3.1	Stochastic wind, 6 seeds, $V_{\text{hub}} = 7$ m/s, $\sigma_{\text{u}} = 1.17$ m/s, $\sigma_{\text{v}} = 0.94$ m/s, $\sigma_{\text{w}} = 0.58$ m/s, no wind shear	Power production, periodic time series solution, $T = 600$ s for each wind seed
3.2b seed 1–6	as in LC 3.1	Stochastic wind, 6 seeds, $V_{\text{hub}} = 13$ m/s, $\sigma_{\text{u}} = 1.83$ m/s, $\sigma_{\text{v}} = 1.46$ m/s, $\sigma_{\text{w}} = 0.92$ m/s, no wind shear	as in LC 3.2a
3.2c seed 1–6	as in LC 3.1	Stochastic wind, 6 seeds, $V_{\text{hub}} = 18$ m/s, $\sigma_{\text{u}} = 2.44$ m/s, $\sigma_{\text{v}} = 1.96$ m/s, $\sigma_{\text{w}} = 1.22$ m/s, no wind shear	as in LC 3.2a
3.2d seed 1–6	as in LC 3.1	Stochastic wind, 6 seeds, $V_{\text{hub}} = 16$ m/s, $\sigma_{\text{u}} = 2.11$ m/s, $\sigma_{\text{v}} = 1.69$ m/s, $\sigma_{\text{w}} = 1.06$ m/s, no wind shear	as in LC 3.2a
4.1	Flexible RNA and tower, 6 DOFs constrained at tower bottom	Steady, deterministic wind, changing from $V_{\text{cut-in}} = 3$ m/s to $V_{\text{cut-out}} = 30$ m/s with step of 1 m/s lasting for 50 s, no wind shear	Power production, periodic time series solution, $T = 1400$ s
4.2c seed 1–6	as in LC 4.1	Stochastic wind, 6 seeds, $V_{\text{hub}} = 18$ m/s, $\sigma_{\text{u}} = 2.44$ m/s, $\sigma_{\text{v}} = 1.96$ m/s, $\sigma_{\text{w}} = 1.22$ m/s, no wind shear	Power production, periodic time series solution, $T = 600$ s for each wind seed
4.2d seed 1–6	as in LC 4.1	Stochastic wind, 6 seeds, $V_{\text{hub}} = 16$ m/s, $\sigma_{\text{u}} = 2.11$ m/s, $\sigma_{\text{v}} = 1.69$ m/s, $\sigma_{\text{w}} = 1.06$ m/s, no wind shear	as in LC 4.2c

V_{hub} – mean wind speed at the hub height
$V_{\text{cut-in}}$ – cut-in wind speed
$V_{\text{cut-out}}$ – cut-out wind speed
θ – blade pitch angle
ϕ – rotor azimuth angle
LAT – lowest astronomical tide
T – simulation time
σ_{u} – standard deviation of longitudinal wind component
σ_{v} – standard deviation of lateral wind component
σ_{w} – standard deviation of vertical wind component

In LC group 1, mass, resulting vertical force, and resulting fore-aft and side-to-side overturning moments were examined at the tower bottom (LC 1a), at four jacket legs around the seabed (LC 1b), and at the bottom of four foundation piles (LC 1c).

In LC group 2, modal properties were examined for the coupled system consisting of the RNA and the support structure with different boundary conditions. In LC 2a, the RNA and tower were modeled as flexible and 6 degrees of freedom (DOFs) were constrained at the tower bottom. In LC 2b, the RNA, tower, TP, and jacket substructure were modeled as flexible and 6 DOFs were constrained at four jacket legs around the seabed. In LC 2c, the entire OWT including its piles was modeled as flexible and participants could model foundation stiffness by the apparent fixity method or alternatively by applying p-y curves along the foundation piles. In LC 2d, the TP and jacket substructure were set as flexible with four jacket legs constrained around the seabed, whereas the tower and the RNA were rigid.

LC groups 3 and 4 were meant for verification of the turbine controller and aerodynamic forces. In the former group, the RNA and tower are modeled as rigid, whereas in the latter as flexible. In LCs 3.1 and 4.1, the stepped deterministic wind is applied to investigate transient response of the system at all operating wind speeds from $V_{\text{cut-in}}$ of 3 m/s to $V_{\text{cut-out}}$ of 30 m/s. In LCs 3.2a,b,c, and d and LCs 4.2c and d turbine response and controller performance were analyzed with turbulent wind at different operating wind speeds, below rated, around rated, and above rated, respectively.

In all verification LCs the marine environment was disregarded. This means that such features as waves, tides, currents, buoyancy force, marine growth, and flooded elements were not accounted for in the analysis. However, such features will be included in the subsequent validation part of OC5 Phase III.

Turbulent wind fields using a Kaimal spectrum were generated at NREL for LC groups 3.2 and 4.2 based on the specification from [15]. It was decided to use six independent wind seeds, each 10 minutes long, for every single LC in order to get statistically comparable results as recommended in the IEC 61400-1 standard [18]. The stochastic wind files could also be generated individually by those participants, whose tools are not able to utilize the provided wind fields due to a different grid format (i.e., Flex5 utilizes a polar grid).

Different components of the OWT were modeled as flexible or rigid depending on the LC type. Environmental loads were applied depending on the definition of the given LC. For each LC, the outputs were recorded at a number of nodal points denoted as sensors located at the RNA and the tower, as shown in Fig. 2. The location of outputs was chosen to capture the global response of the OWT.

Start-up transients were removed by using a presimulation time, T_{pre}, which is simulated but cut-out from the result files in all simulations. T_{pre} was not explicitly defined. It was chosen individually by each participant in order to avoid initial numerical transients and to satisfy the initial conditions of the given LC. The time step for data output was defined as $\Delta t = 0.05$ s for all LCs.

DATA POSTPROCESSING AND ANALYSIS METHODS

All simulation results were delivered by the project participants in terms of time series data. Their post processing was performed internally at Fraunhofer IWES in Matlab and MCrunch [19].

LCs with deterministic wind were visually compared in

terms of their time series. The results accuracy was checked by the nondimensional root mean square error (RMSE). The RMSE can be used as a measure of the difference between time series data points, X_t, predicted by every single OC5 Phase III model and the time series data points, $X_{\mathrm{SWE},t}$, obtained from the reference SWE model. These individual differences, at each time step, t, are aggregated by the RMSE into a single value. The RMSE is defined as the square root of the mean squared error divided over the number of the data points, n, in the analyzed time series:

$$\mathrm{RMSE} = \sqrt{\frac{\sum_{t=1}^{n} (X_t - X_{\mathrm{SWE},t})^2}{n}} \tag{1}$$

It has to be noted that the RMSE:

- Is not the 'ultimate measure' for assessment of accuracy. The time series results that are phase shifted from the SWE reference time series get larger errors compared to those that are in phase. Therefore, the RMSE should not be interpreted in separation from the time series plots.
- Gives a relatively high weight to large errors as they are squared before they are averaged. Therefore, higher discrepancies between the reference SWE model and the OC5 Phase III models are penalized more by this statistical measure.

A nondimensional form of the RMSE is obtained by normalizing the RMSE to the range of the reference data set $X_{\mathrm{SWE,max}} - X_{\mathrm{SWE,min}}$. The NRMSE is expressed as a percentage, where lower values indicate less residual variance and therefore a better fit:

$$\mathrm{NRMSE} = \frac{\mathrm{RMSE}}{X_{\mathrm{SWE,max}} - X_{\mathrm{SWE,min}}} 100\% \tag{2}$$

LCs with turbulent wind were examined in terms of probability density functions (PDFs) and power spectral densities (PSDs). PSDs and PDFs are computed from six aggregated time series, each 10 minutes long.

SELECTED RESULTS

This section presents example results of the OWT models verification against the reference model consisting of the Senvion 5M wind turbine and the jacket support structure from OWEC Tower, which was implemented in the Flex5-Poseidon at SWE. Information about Flex5-Poseidon can be found in [20]. This encrypted model contains a detailed description of the entire OWT including structural and aerodynamic properties of the blades designed by LM Wind Power and the fully functional controller from Senvion. It should be noted that SWE also participates in Phase III with another simulation tool—Simpack. The Simpack OWT model is based only on the OC5 Phase III specification [11] and should not be confused with the reference OWT model implemented in Flex5-Poseidon.

Presented results give a general overview of differences between the reference SWE model and the OC5 Phase III models. The results discussed in this paper represent the final outcome of multiple modelling iterations that were necessary to develop numerical models of the OWT, which are adequate for further validation needs. During each modelling iteration, the participants updated their OWT models to better match with the solutions from the reference SWE model and documentation provided by Senvion and OWEC Tower.

Comparison of Mass and Overturning Moments

Verification of different implementations of the OWT model against the reference SWE model is performed by comparing masses and fore-aft overturning moments at the tower base or at the bottom of foundation piles, respectively. Mass and moments would give a rough idea whether the structural properties of the turbine are correctly implemented. Mass distribution would have a direct impact on structural dynamics. High discrepancies in the overturning moment would indicate issues with center of gravity (CG) of different system components and/or incorrect stiffness distribution.

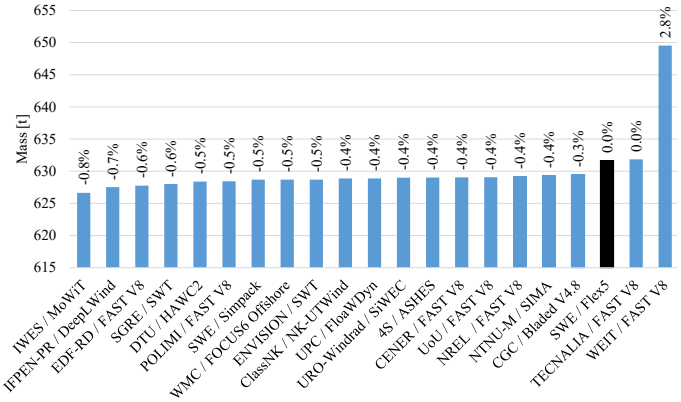

FIGURE 3: LC 1A – MASS OF THE RNA AND TOWER

The example results for LCs 1a and 1c are shown in Figs. 3–5. Reference values of the SWE model are denoted with black bars. The results of the Phase III participants are marked with blue bars and sorted in increasing order from left to right. The percentage change with respect to the SWE (Flex5) value is added at the top of each bar. A missing bar indicates that the results were not provided by the given participant for this particular LC. A very good match of the RNA and tower mass is observed for all project participants in Fig. 3. A small discrepancy is visible in the case of WEIT (FAST V8), as this participant did

not use the most recent specification of the tower model which included the updated value of the material density.

Also, a very good match between the majority of the models and the reference SWE model is observed in the case of the fore-aft overturning moment, M_y, at the tower bottom in Fig. 4. Larger discrepancies might indicate misplaced CG of some of the RNA components. The increase of M_y would indicate that the CG of the RNA is shifted upwind from the central vertical axis of the tower. The reduced M_y would indicate the opposite—CG shifted downwind toward the tower center.

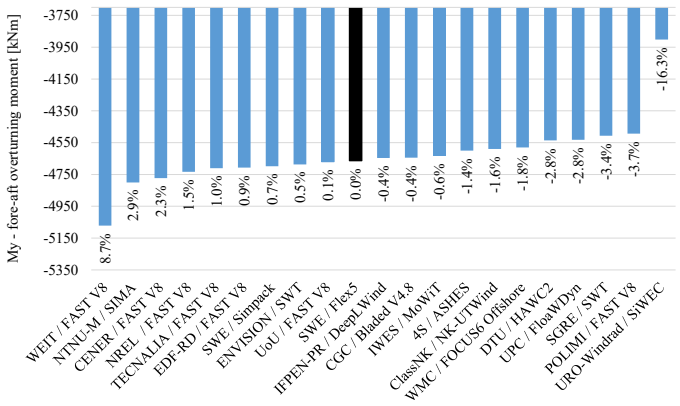

FIGURE 4: LC 1A – FORE-AFT OVERTURNING MOMENT AT THE TOWER BOTTOM

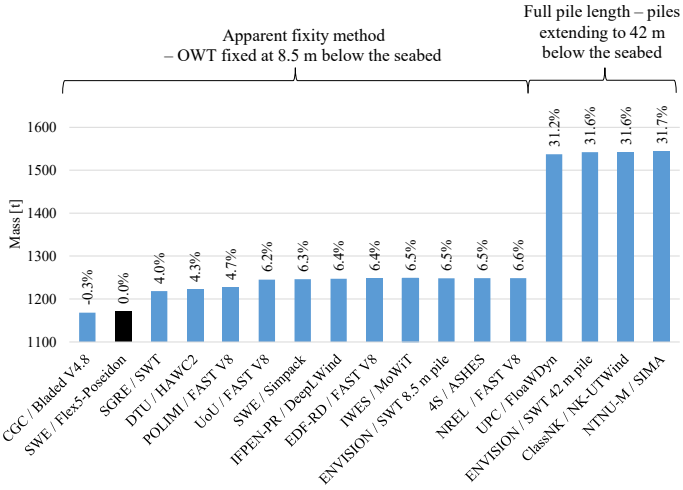

FIGURE 5: LC 1C – MASS OF THE ENTIRE OWT INCLUDING RNA, TOWER, TP, JACKET SUBSTRUCTURE AND FOUNDATION PILES

Figure 5 shows the mass of the RNA, tower, TP, jacket substructure, and foundation piles. The majority of models are heavier, around 3 to 6.5% compared to the reference SWE model. The reason is that the reference SWE model does not include secondary steel masses for the jacket substructure. Those masses were included in models setup within OC5 Phase III. UPC, ENVISION, ClassNK, and NTNU-M models are around 31% heavier than the reference SWE model. The difference comes from the modeling of the foundation piles. The majority of participants followed the modeling approach of SWE and used an apparent fixity model by identifying a shortened (fictitious) pile that extends from the seabed to a clamped point 8.5 m below the seabed that mimics the flexibility of the real pile penetrating the soil. The remaining four participants modeled the full length of the real pile extending to 42 m below the seabed and used p-y curves provided by OWEC Tower for pile-soil interaction.

Summing up, a very good match between the reference SWE model and the OC5 Phase III models was achieved in terms of mass and overturning moments.

Eigenanalysis

Four LCs were defined for eigenmode analysis in Tab. 3. Some results for LC 2b are shown in Fig. 6. The eigenanalysis was performed for the flexible RNA, tower, TP, and the jacket substructure with 4 legs constrained at LAT -29.5 m.

The results for the first global fore-aft mode average around 2% lower compared to the reference SWE model, as shown in Fig. 6a. The secondary steel masses, which are included in the OC5 Phase III models, might be responsible for this general trend. Note that the reference SWE model is slightly lighter, as it does not include secondary steel masses in the jacket substructure (see Fig. 5).

Figures 6b–6f show diverse coupled modes, which are dominated by flap- and edgewise deflections of the blades. The majority of the participants matched quite well with the SWE reference model. The results are very good considering the fact that the definition of the real blade was not available for the OC5 Phase III project. They prove that OWT models with tuned NREL 5-MW blades can mimic the behavior of the reference SWE model that contains the structural definition of the real blades. Some discrepancies are always expected, as different simulation tools incorporate a different number of DOFs and different ways of modeling the structure. Furthermore, for higher modes, it is challenging to identify which coupled mode is actually induced, purely based on the modes visualization. Figure 7 shows visualizations of the first fore-aft global mode from four arbitrarily chosen tools.

Deterministic Load Cases with Stepped Wind

To investigate the transient response of the system at all operating wind speeds, a stepped wind was increased from $V_{\text{cut-in}}$ to $V_{\text{cut-out}}$ with a step of 1 m/s, lasting for 50 s. Figure 8 shows the rotor speed for LC 3.1 where only the rotor rotational DOF and the pitch system rotational DOF were enabled (see Tab. 3). A rel-

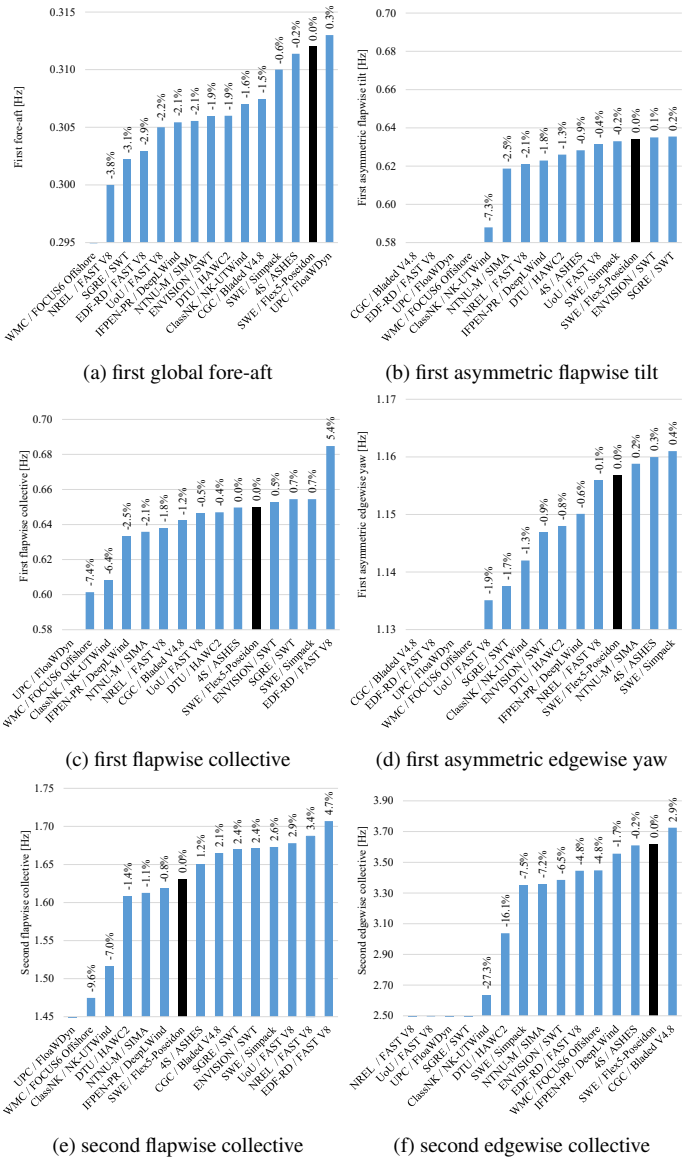

(a) first global fore-aft

(b) first asymmetric flapwise tilt

(c) first flapwise collective

(d) first asymmetric edgewise yaw

(e) second flapwise collective

(f) second edgewise collective

FIGURE 6: LC 2B – SELECTED EIGENFREQUENCIES NAMED ACCORDING TO THE DOMINANT MODES

atively good match of the rotor speed is achieved in the partial-loading region for wind speeds between 6 and 8 m/s, (time between 150 and 250 s, in Fig. 8) and in the full-loading region between 15 and 17 m/s (time between 600 and 750 s in Fig. 8). In the transition region from around 8 to 13 m/s (time between 250 and 550 s in Fig. 8), there are discrepancies due to unavoidable differences in the blade aerodynamics and controller. In this region, the majority of the models reach larger rotational speeds than the reference SWE model, which is denoted with a black, solid curve. Tuning of the NREL blade aerodynamic properties to achieve similar response to the real blade in all operating conditions would be very time consuming, and therefore not doable within the time frame of Phase III. Therefore, the transition operating region will not be used for the intended validation task. Rotor speed oscillations with a time period of 16.1 s are visible in the full-loading region (from around 500 s onward) in the case of CENER, WEIT (both FAST V8), and WMC (Focus6 Offshore). Those participants did not use the most recent version of the pitch proportional-integral-derivative (PID) controller provided by Fraunhofer IWES. POLIMI (FAST V8) reached the rotor rated speed already at the wind speed of 9 m/s. POLIMI decided to adapt the Basic DTU Wind Energy Controller [21] for its own simulations. This controller requires further tuning to match the reference SWE results. The results of the remaining participants match well with the reference SWE results—a sudden increase of the rotor speed caused by a rapid wind speed change is smoothly mitigated by the PID pitch controller.

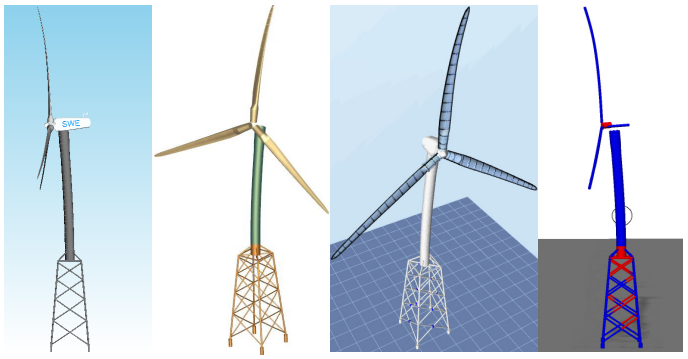

FIGURE 7: LC 2B – FIRST GLOBAL FORE-AFT MODE, FROM LEFT: SWE (SIMPACK) , ENVISION (SWT), 4S (ASHES), NTNU-M (SIMA)

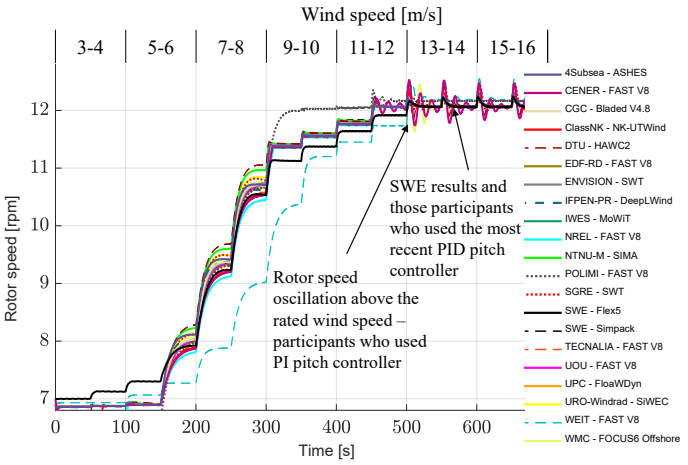

FIGURE 8: LC 3.1 – ROTOR SPEED CHANGING DUE TO DETERMINISTIC STEPPED WIND

Figure 9 shows the fore-aft shear force, F_x, at the tower top

for LC 3.1 (see Tab. 3). The time series is trimmed at the full-loading region for the wind speed of 16 m/s. The force peak at 650 s is caused by the rapid change in the wind speed from 15 to 16 m/s at this particular time point. The majority of the tools match quite well with the maximum peak value from the reference SWE results. Also, their transient decays are comparable to the SWE (Flex5) results. This proves that the tuned pitch PID controller is performing well. Oscillations at 3P frequency due to the tower shadow are visible in the majority of the results. Their frequency and amplitude match the reference SWE results very well. ClassNK (NK-UTWind), UOU (FAST V8), and TECNALIA (FAST V8) do not include the tower shadow in their simulations. Note that the SGRE (SWT) results are not visible, as they were around two times larger compared to other codes, though the oscillation pattern seemed to match the other simulation tools well.

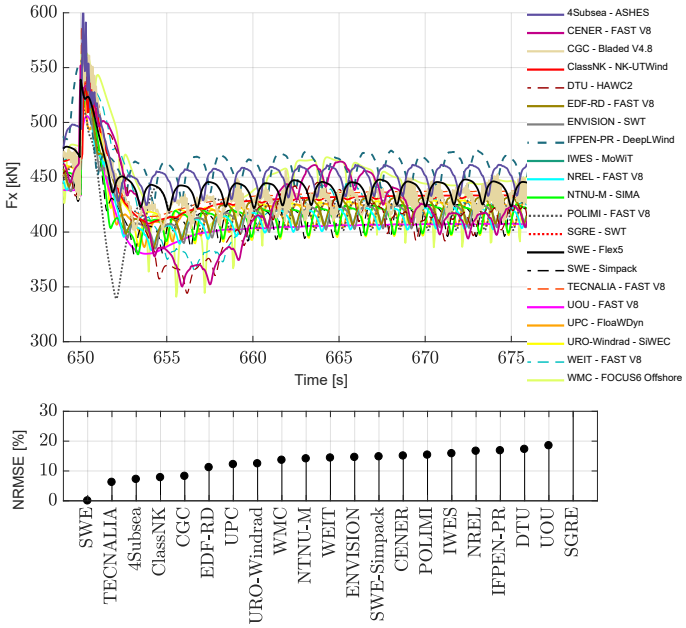

FIGURE 9: LC 3.1 – TOWER TOP FORE-AFT SHEAR FORCES AND NRMSE – DETERMINISTIC WIND SPEED OF 16 M/S

The NRMSE is shown below the time series in Fig. 9. The values are sorted left to right in ascending order—from the best fit to the worse. The NRMSE varies between 6 and 15% for the majority of the participants, which is considered to be a very good result.

Figures 10 and 11 show the tower top fore-aft displacement, x, in the partial- and the full-loading region, respectively, for LC 4.1 (see Tab. 3). In LC 4.1, the RNA and tower are flexible. Likewise, in LC 3.1, the stepped wind is applied from $V_{\text{cut-in}}$ to $V_{\text{cut-out}}$. Mean values of the displacement match quite well with the reference SWE model. Tower fore-aft displacement oscillations with a time period of around 2.7 s (0.375 Hz) corresponding to the first fore-aft global mode are visible in all the results. Note that the results of WEIT (FAST V8) are shifted in time—the stepped wind speed was applied with a delay of 50 s with respect to other results. Note that POLIMI (FAST V8) results are not depicted in Fig.11 due to the severe oscillations caused by the controller. The NRMSE values are shown in ascending order below the time series in Figs. 10 and 11. The NRMSE varies between 6 and 15% for the majority of the participants, which is considered to be a very good match.

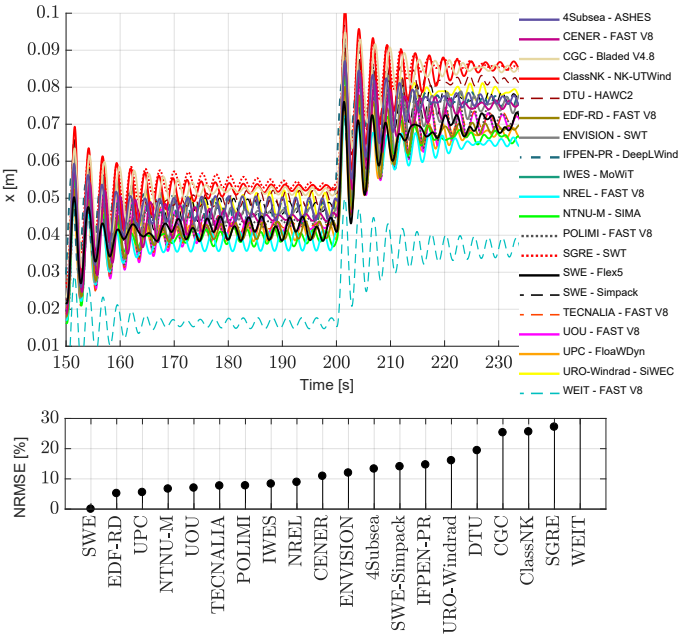

FIGURE 10: LC 4.1 – TOWER TOP FORE-AFT DISPLACEMENTS AND NRMSE – DETERMINISTIC WIND SPEEDS OF 6 AND 7 M/S

Stochastic Load Cases at Selected Operating Points

Stochastic LCs are analyzed in terms of PSD and PDF plots, which were created from an aggregated time series of 6 independent seeds for each data set.

Figure 12 shows the PSD and PDF of the pitch angle for LC 3.2d (see Tab. 3). Probability distributions of the majority of the OWT models set up within OC5 Phase III match well with the reference SWE model—denoted with the black, solid curve. This proves that the tuned controller performs well. Subsequent rotor harmonics, such as 3P, 6P and 9P are visible in PSD plots for the majority of the results. Some discrepancies are visible in PSD plots of DTU (HAWC2) and UPC (FloaWDyn) results. Even though DTU used the most recent controller, there is a discrepancy in their results. The energy spectrum of the DTU results is relatively flat from around 2 Hz—probably due to the provided controller parameters that are not optimized for the

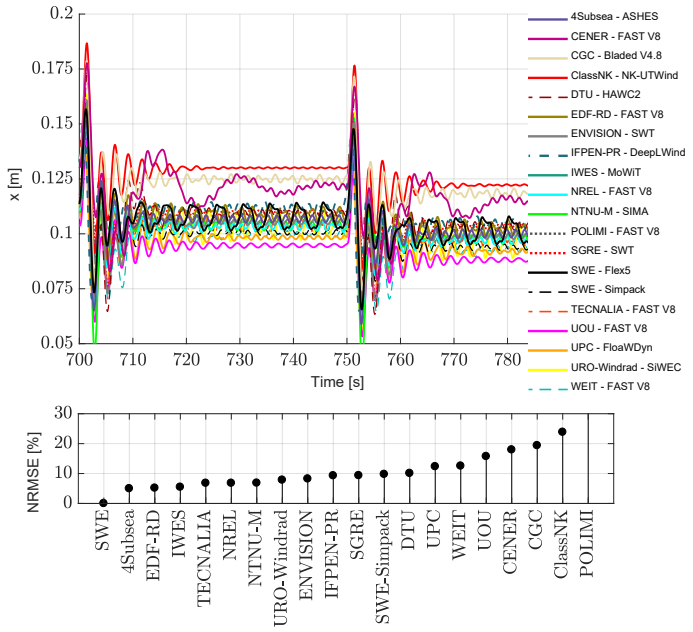

FIGURE 11: LC 4.1 – TOWER TOP FORE-AFT DISPLACEMENTS AND NRMSE – DETERMINISTIC WIND SPEEDS OF 17 AND 18 M/S

structural model in HAWC2.

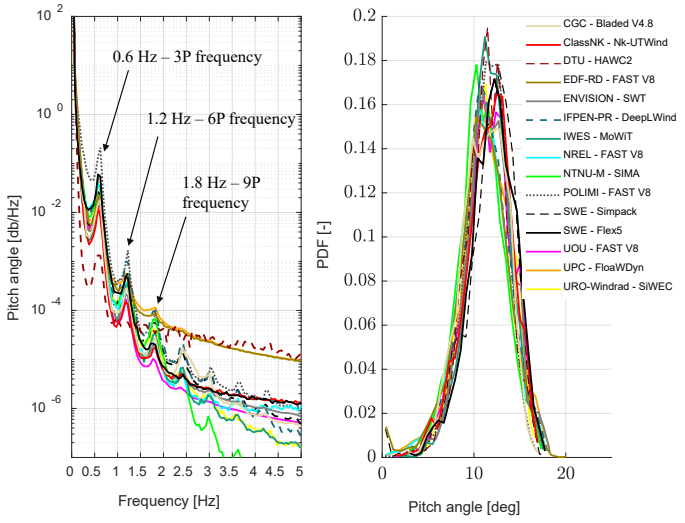

FIGURE 12: LC 3.2D – PSD AND PDF OF PITCH ANGLE FOR TURBULENT WIND WITH A MEAN WIND SPEED OF 16 M/S

Figure 13 shows the PSD and PDF plots of the fore-aft overturning moment, M_y, at the tower bottom for LC 4.2d (see Tab. 3). Probability distributions of the majority of tools match relatively well with the reference SWE model. Some discrepancies are visible in the case of POLIMI (FAST V8) results, where probability distributions are much flatter compared to other results. The reason is that POLIMI did not use the provided DLL controller. In the PSD results, energy peaks are visible at the frequencies corresponding to the first fore-aft global mode, and flap- and edgewise modes. Higher frequency peaks at around 3.4 Hz, 3.7 Hz, and 4.4 Hz are visible in the SWE (Flex5) results and in the results of some participants. Those peaks correspond to two different second blade edgewise modes and the tower second fore-aft mode, respectively. Note that the second edgewise mode is not reproduced by FAST V8 models that do not use the BeamDyn nonlinear FEM-based blade structural-dynamics module.

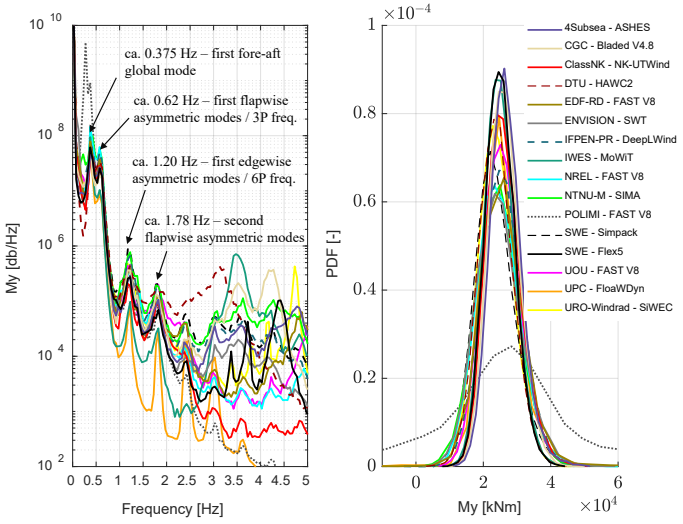

FIGURE 13: LC 4.2D – PSD AND PDF OF FORE-AFT BENDING MOMENT AT TOWER BOTTOM FOR TURBULENT WIND WITH A MEAN WIND SPEED OF 16 M/S

CONCLUSIONS

The verification process was quite challenging as the real blade design data and the full controller were not available to the OC5 Phase III participants due to confidentiality. It was also not the aim to do a detailed re-engineering of the blade structural and aerodynamic properties, and design of the state-of-the-art controller that would be able to compete with the proprietary Senvion 5M controller. Tuning was done on a reasonable level considering the selected loading scenarios that were used for the comparison. The subsequent validation task will be mostly focused on the support structure. Therefore, the most important task was to obtain adequate system responses, such as displacements and forces for the support structure components.

Based on the provided data, OC5 Phase III participants set up their models and verified them against the reference SWE model set up in Flex5-Poseidon, which included a definition of the real blade and the fully functional Senvion 5M controller.

Due to the differences in blade aerodynamics between the tuned NREL 5-MW blades (utilized in OC5 Phase III) and Senvion 5M reference turbine model in Flex5-Poseidon (available for comparison at SWE), it was not possible to obtain a comparable system response at all operating regions of the turbine. Nevertheless, a satisfactory response could be achieved in the partial- and full-loading regions for wind speeds between 6 and 8 m/s, and 15 and 17 m/s, respectively. Therefore, verification and validation can be performed at these ranges of operating wind speeds. In those operating regions, the relatively low NRMSE values in the range between 6 and 15% were achieved for the analyzed outputs between the OC5 Phase III models and the reference SWE model for the majority of the participants. It has to be noted that the NRMSE gives a relatively high weight to large errors—other statistical measures might provide an even better fit.

The goal is to now move forward with validation against the measurements from the alpha ventus wind farm, using the models developed.

ACKNOWLEDGEMENTS

OWEC Tower is acknowledged for releasing the jacket support structure design data for Phase III. Friedemann Borisade from University of Stuttgart, SWE is acknowledged for engaging the SWE team in the verification process with the reference OWT model in Flex5-Poseidon. Dr. Fanzhong Meng from Fraunhofer IWES is acknowledged for his help in tuning of the control parameters of the NREL 5-MW controller.

The Alliance for Sustainable Energy, LLC (Alliance) is the manager and operator of NREL. NREL is a national laboratory of the U.S. Department of Energy, Office of Energy Efficiency and Renewable Energy. This work was authored by the Alliance and supported by the U.S. Department of Energy under Contract No. DE-AC36-08GO28308. Funding was provided by the Wind and Water Power Program. The views expressed in the article do not necessarily represent the views of the U.S. Department of Energy or the U.S. government. The U.S. government retains, and the publisher, by accepting the article for publication, acknowledges that the U.S. government retains a nonexclusive, paid-up, irrevocable, worldwide license to publish or reproduce the published form of this work, or allow others to do so, for U.S. government purposes.

REFERENCES

[1] Musial, W., Robertson, A., Jonkman, J., Vorpahl, F., and Popko, W., 2013. Annex 30 – Task Extension Proposal, 2014–2017 Offshore Code Comparison Collaboration Continuation (OC4). Tech. rep., International Energy Agency, September.

[2] Jonkman, J., and Musial, W., 2010. IEA Wind Task 23 Offshore Wind Technology and Deployment. Tech. Rep. NREL/TP-5000-48191, National Renewable Energy Laboratory, Golden, CO, December. See also URL https://www.nrel.gov/docs/fy11osti/48191.pdf.

[3] Robertson, A., Jonkman, J., Musial, W., Popko, W., and Vorpahl, F., 2014. Final Technical Report – IEA Wind Task 30 Offshore Code Comparison Collaboration Continued. Tech. rep., The International Energy Agency Wind, April. See also URL http://www.ieawind.org/index_page_postings/task30/Task30_Final_Technical_Report.pdf.

[4] Robertson, A. N., Wendt, F., Jonkman, J. M., Popko, W., Borg, M., Bredmose, H., Schlutter, F., Qvist, J., Bergua, R., Harries, R., Yde, A., Nygaard, T. A., de Vaal, J. B., Oggiano, L., Bozonnet, P., Bouy, L., Sanchez, C. B., Garca, R. G., Bachynski, E. E., Tu, Y., Bayati, I., Borisade, F., Shin, H., van der Zee, T., and Guerinel, M., 2016. "OC5 Project Phase Ib: Validation of Hydrodynamic Loading on a Fixed, Flexible Cylinder for Offshore Wind Applications". *Energy Procedia,* ***94***, September, pp. 82–101. See also URL http://dx.doi.org/10.1016/j.egypro.2016.09.201.

[5] Robertson, A. N., Wendt, F., Jonkman, J. M., Popko, W., Dagher, H., Gueydon, S., Qvist, J., Vittori, F., Azcona, J., Uzunoglu, E., Soares, C. G., Harries, R., Yde, A., Galinos, C., Hermans, K., de Vaal, J. B., Bozonnet, P., Bouy, L., Bayati, I., Bergua, R., Galván, J., Mendikoa, I., Sanchez, C. B., Shin, H., Oh, S., Molins, C., and Debruyne, Y., 2017. "OC5 Project Phase II: Validation of Global Loads of the DeepCwind Floating Semisubmersible Wind Turbine". *Energy Procedia,* ***137***, October, pp. 38–57. See also URL https://doi.org/10.1016/j.egypro.2017.10.333.

[6] Wikipedia, 2009. Lage und Detailkarte des Windparks Alpha Ventus in der Nordsee [in German], January. See also URL https://de.wikipedia.org/wiki/Alpha_ventus#/media/File:Windpark_alpha_ventus_Lagekarte.png.

[7] BINE Information Service, 2012. BINE Informationsdienst: Themeninfo: RAVE – Forschen am Offshore-Testfeld – Wind Turbine Technology and Components, January. See also URL http://www.bine.info/en/publications/themeninfos/publikation/rave-forschen-am-offshore-testfeld/anlagentechnik-und-komponenten/.

[8] Kaufer, D., and Cheng, P. W., 2014. "Validation of an Integrated Simulation Method with High Resolution Load Measurements of the Offshore Wind Turbine REpower 5M at Alpha Ventus". *Journal of Ocean and Wind Energy,* ***1***(1), February, pp. 30–40. See also URL http://www.isope.org/publications/jowe/jowe-01-1/JOWE-01-1-p030-arr01-Kaufer.pdf.

[9] Müller, K., Reiber, M., and Cheng, P., 2016. "Comparison of Measured and Simulated Structural Loads of an Offshore Wind Turbine at Alpha Ventus". *Interna-*

tional Journal of Offshore and Polar Engineering, ***26***(3), pp. 209–218. See also URL https://www.onepetro.org/journal-paper/ISOPE-16-26-3-209.

[10] Fraunhofer IWES, 2017. OWEA Loads – Probabilistic Load Description, Monitoring and Reduction of Loads of Future Offshore Wind Turbines. See also URL http://rave-static.iwes.fraunhofer.de/en/projects/owea_loads/.

[11] Popko, W., 2017. OC5 Phase III – RNA and Tower Definition [Confidential]. Tech. rep., Fraunhofer Institute for Wind Energy Systems IWES, Bremerhaven, December.

[12] Jonkman, J., Butterfield, S., Musial, W., and Scott, G., 2009. Definition of a 5-MW Reference Wind Turbine for Offshore System Development. Tech. Rep. NREL/TP-500-38060, National Renewable Energy Laboratory, Golden, CO, February. See also URL http://www.nrel.gov/docs/fy09osti/38060.pdf.

[13] Kooijman, H. J. T., Lindenburg, C., Winkelaar, D., and van der Hooft, E. L., 2003. DOWEC 6 MW PRE-DESIGN Aero-elastic Modelling of the DOWEC 6 MW Pre-design in PHATAS. Tech. Rep. ECN-CX–01-135, ECN, September. See also URL http://www.ecn.nl/fileadmin/ecn/units/wind/docs/dowec/10046_009.pdf.

[14] Dubois, J., Muskulus, M., and Schaumann, P., 2013. "Advanced Representation of Tubular Joints in Jacket Models for Offshore Wind Turbine Simulation". *Energy Procedia,* ***35***, pp. 234–243.

[15] Popko, W., 2017. OC5 Phase III – Verification of OWT Model [Confidential]. Tech. rep., Fraunhofer Institute for Wind Energy Systems IWES, Bremerhaven, December.

[16] Passon, P., Kühn, M., Butterfield, S., Jonkman, J., Camp, T., and Larsen, T. J., 2007. "OC3 – Benchmark Exercise of Aero-elastic Offshore Wind Turbine". *Journal of Physics: Conference Series,* ***75***(1), August, p. 12. See also URL http://dx.doi.org/10.1088/1742-6596/75/1/012071.

[17] Popko, W., Vorpahl, F., Zuga, A., Kohlmeier, M., Jonkman, J., Robertson, A., Larsen, T. J., Yde, A., Sætertrø, K., Okstad, K. M., Nichols, J., Nygaard, T. A., Gao, Z., Manolas, D., Kim, K., Yu, Q., Shi, W., Park, H., Vásquez-Rojas, A., Dubois, J., Kaufer, D., Thomassen, P., de Ruiter, M. J., van der Zee, T., Peeringa, J. M., Zhiwen, H., and von Waaden, H., 2014. "Offshore Code Comparison Collaboration Continuation (OC4), Phase I – Results of Coupled Simulations of an Offshore Wind Turbine with Jacket Support Structure". *Journal of Ocean and Wind Energy,* ***1***(1), February, pp. 1–11. See also URL http://www.isope.org/publications/jowe/jowe-01-1/JOWE-01-1-p001-jcr07-Popko.pdf.

[18] IEC, 2005. *IEC 61400-1 Wind Turbines – Part 1: Design Requirements*, 3 ed. International Electrotechnical Commission, Geneva, August.

[19] Buhl, M., 2008. MCrunch User's Guide for Version 1.00. Tech. Rep. NREL/TP-500-43139, National Renewable Energy Laboratory. See also URL https://nwtc.nrel.gov/MCrunch.

[20] Kaufer, D., Cosack, N., Böker, C., Seidel, M., and Kühn, M., 2009. "Integrated Analysis of the Dynamics of Offshore Wind Turbines with Arbitrary Support Structures". In Proceedings of European Wind Energy Conference 2009, Marseille, European Wind Energy Association.

[21] Hansen, M. H., and Henriksen, L. C., 2013. Basic DTU Wind Energy Controller. Tech. Rep. DTU Wind Energy E-0018, DTU Wind Energy, January. See also URL http://orbit.dtu.dk/files/56263924/DTU_Wind_Energy_E_0028.pdf.